J Mater Sci: Mater Med (2010) 21:2569–2581
DOI 10.1007/s10856-010-4119-0

Design of novel three-phase PCL/TZ–HA biomaterials for use in bone regeneration applications

Aurelio Salerno · Maria Oliviero · Ernesto Di Maio · Paolo A. Netti · Cristina Rofani · Alessia Colosimo · Valentina Guida · Bruno Dallapiccola · Paolo Palma · Emidio Procaccini · Anna C. Berardi · Francesco Velardi · Anna Teti · Salvatore Iannace

Received: 18 December 2009 / Accepted: 22 June 2010 / Published online: 2 July 2010
© Springer Science+Business Media, LLC 2010

Abstract The design of bioactive scaffold materials able to guide cellular processes involved in new-tissue genesis is key determinant in bone tissue engineering. The aim of this study was the design and characterization of novel multi-phase biomaterials to be processed for the fabrication of 3D porous scaffolds able to provide a temporary biocompatible substrate for mesenchymal stem cells (MSCs) adhesion, proliferation and osteogenic differentiation. The biomaterials were prepared by blending poly(ε-caprolactone) (PCL) with thermoplastic zein (TZ), a thermoplastic material obtained by de novo thermoplasticization of zein. Furthermore, to bioactivate the scaffolds, microparticles of osteoconductive hydroxyapatite (HA) were dispersed within the organic phases. Results demonstrated that materials and formulations strongly affected the microstructural properties and hydrophilicity of the scaffolds and, therefore, had a pivotal role in guiding cell/scaffold interaction. In particular, if compared to neat PCL, PCL–HA composite and PCL/TZ blend, the three-phase PCL/TZ–HA showed improved MSCs adhesion, proliferation and osteogenic differentiation capability, thus demonstrating potential for bone regeneration.

1 Introduction

The repair and reconstruction of bone skeletal defects by traditional medical treatments, like autologous or allogenic bone graft, are often impaired by the complexity of the procedures involved, as well as due to donor site scarcity,

A. Salerno (✉) · P. A. Netti
Interdisciplinary Research Centre on Biomaterials (CRIB) and Italian Institute of Technology (IIT), Piazzale Tecchio 80, 80125 Naples, Italy
e-mail: asalerno@unina.it

A. Salerno · M. Oliviero · S. Iannace
Institute of Composite and Biomedical Materials, National Research Council (IMCB-CNR), Piazzale Tecchio 80, 80125 Naples, Italy

E. Di Maio · P. A. Netti
Department of Materials and Production Engineering, University of Naples Federico II, Piazzale Tecchio 80, 80125 Naples, Italy

C. Rofani · A. C. Berardi
Stem Cells Laboratory, Bambino Gesù Children's Hospital, Scientific Institute (IRCCS), Rome, Italy

A. Colosimo
Department of Comparative Biomedical Science, University of Teramo, Teramo, Italy

V. Guida · B. Dallapiccola
IRCCS-CSS San Giovanni Rotondo and CSS Mendel Institute, Rome, Italy

V. Guida · B. Dallapiccola
Department of Experimental Medicine and Pathology, University "La Sapienza", Rome, Italy

P. Palma · E. Procaccini · F. Velardi
Neurosurgery, Bambino Gesù Children's Hospital, Scientific Institute (IRCCS), Rome, Italy

A. Teti
Department of Experimental Medicine, University of L'Aquila, L'Aquila, Italy

foreign body reactions and pathogen transfer occurrence [1–4]. Furthermore, these treatments are often inadequate for a large number of clinical needs, such as bone repair in paediatric-age patients, because of the continuous growth and remodelling of bone structures [5].

In the past 20 years, tissue engineering has emerged as an alternative and very promising approach for the regeneration of biological tissues, including bone and cartilage. In this approach, transplanted cells are expanded in vitro and seeded onto a scaffold and, subsequently implanted in vivo in the defect site [3, 4].

A large number of studies highlighted the possibility of using multipotent bone marrow-derived mesenchymal stem cells (MSCs) for orthopedic and craniofacial tissue engineering applications, rather than committed osteoblasts [6–8]. Indeed, MSCs may be candidate cells for tissue engineering and regenerative therapies for their ability to differentiate into a variety of connective tissue lineages, including bone and cartilage, as well as for their potential of expansion, and lineage-specific differentiation when combined with autologous sources [6, 7]. Additionally, in vivo studies demonstrated that MSCs were able to produce bone tissue when encased in tissue-specific scaffolds and implanted into different tissue sites [8].

Several biodegradable material scaffolds, in particular ceramics and polymers of natural or synthetic origins, have been investigated for bone repair and regeneration [3, 4, 9, 10]. Ceramics, such as hydroxyapatite (HA), have been widely used in the biomedical engineering and bone regeneration in view of their osteoconductive and osteoinductive properties [3, 9, 10]. Furthermore, ceramics allowed the design of scaffolds with a mechanical function suitable for bone repair [10]. To improve their processability, ceramics have been mixed with synthetic polymers as inorganic filler, in form of particles of different size and shape [11–13]. Despite the advantages offered by polymer/ceramic composites, these materials showed limited control over cell biosynthesis and new-tissue regeneration, probably due to the un-complete and un-efficient exposure of the particles to bone cells and tissues [14]. This is a very important aspect, especially at the early stage of in vitro and/or in vivo applications of high hydrophobic polymers, such as poly(ε-caprolactone) (PCL), because the polymeric matrix requires very long times to degrade and to allow for the complete exposure of the ceramic particles [4, 14].

Blending synthetic and natural polymers may be a very efficient way to overcome these limitations and to enhance the control over the degradation of polymeric scaffolds [15, 16]. Furthermore, with respect to synthetic polymers, naturally derived ones may have the potential advantages of specific cell interactions and improved hydrophilicity and, therefore, may enhance cell seeding, proliferation and, in such cases, the osteogenic differentiation of stem cells [14, 15].

Among the natural biopolymers, zein, a major storage protein of corn, has been investigated for tissue engineering applications [17, 18]. Zein scaffolds showed bone regeneration capabilities, promoting MSCs adhesion, proliferation and osteogenic differentiation [18]. With respect to other biopolymers, such as gelatin, zein is characterized by a higher hydrophobic amino acids content [17] and, a corresponding reduced dissolution in water. For these reasons, zein has been used for tissue engineering applications without any additional cross-linking processes, otherwise necessary for retarding the dissolution rate of others proteins, such as gelatin [19] and, potentially harmful for cells and tissues [20].

We recently reported that, when thermoplasticized with poly(ethylene glycol), zein allowed for the formation of a thermoplastic material (thermoplastic zein, TZ) suitable to be melt processed and gas foamed for the preparation of 3D porous materials [21].

In this work we prepared novel multi-phase PCL/TZ blend and PCL/TZ–HA composite for bone regeneration. The physicochemical properties of these biomaterials were evaluated and compared to those of neat PCL and PCL–HA composite. In particular, thermogravimetric analysis (TGA), dynamic mechanical analysis (DMA) and tensile test were performed in order to assess the thermal stability, the viscoelastic behavior and the mechanical response of the systems. Furthermore, the effect of blend composition on the hydrophilic properties and degradation of the different biomaterials was investigated by contact angle measurement and in vitro degradation analysis and the results were correlated with scaffold morphologies at different degradation intervals.

Bone marrow derived rabbit mesenchymal stem cells (rMSCs) were seeded onto non-porous scaffolds to evaluate their biological response. To this purpose, DNA measurements were performed at 1, 7 and 21 days of culture in order to assess rMSCs adhesion and proliferation. Furthermore, Alkaline phosphatase activity (ALP), Alizarin red staining (ARS) and Osteopontin expression (OPN) tests were performed at 21 days of culture to assess the rMSCs osteogenic differentiation and calcium deposition.

2 Materials and methods

2.1 Materials

PCL (MW = 65 kDa, T_m = 59–64°C and T_g = −60°C) and maize zein powder (cod.: Z3625, batch: 065K0110) were purchased from Sigma–Aldrich (Italy). Poly(ethylene glycol) (PEG) 400 was purchased by Fluka (Italy) and used

as plasticizer for the preparation of the TZ. HA granules (ENGIpore, batch 071105, 250–355 μm size) were purchased from Finceramica (Faenza, Italy).

2.2 Biomaterial scaffolds preparation

The TZ was prepared as described in details in a previous reported work [21]. The biomaterials were prepared by using a twin counter rotating internal mixer connected to a control unit (Rheomix 600 and Rheocord 9000, respectively, Haake, Germany), at 70°C, 80 rpm for 6 min. PCL pellets were first melted at 70°C, 20 rpm for 2 min and, subsequently, TZ and/or HA were added into the mixing chamber and mixed at 80 rpm for 6 min. Mixing compositions are reported in Table 1. Finally, the biomaterials were compression molded at 80°C and 30 bar into 1 or 2 mm-thick plates by a hot press (P300P, Collin, Germany).

2.3 Characterization of the physical properties and in vitro degradation of the biomaterials

TGA was performed to evaluate the thermal stability of the different biomaterials prepared. In particular, TGA experiments were carried out on a TGA 2950 (TA Instruments, USA) over a 30–600°C temperature range at 10°C/min under inert atmosphere.

The dynamic-mechanical properties of the different biomaterials were determined by using a DMA Tritec 2000 (Triton technology, Ltd. UK). Rectangular samples (length = 8 mm, width = 27 mm and thickness = 1 mm) were tested in a dual cantilever bending mode, at an oscillatory frequency of 1 Hz and in the −130 to 50°C temperature range (2°C/min heating rate). The TGA and DMA analyses of neat TZ were also performed for comparison.

Tensile tests were performed at room temperature according to ASTM standard D1708-02 by using a 4204 Universal Testing Machine (Instron, USA) equipped with a 1 kN load cell. Force and displacement were measured by the apparatus and recorded to evaluate yielding stress (σ_Y), stress at break (σ_B) and elongation at break (ε_B). Five samples for each composition were tested.

Table 1 Biomaterials formulation

Scaffold formulations	PCL content (wt%)	TZ content (wt%)	HA content (wt%)
PCL	100	–	–
PCL–HA	80	–	20
PCL/TZ	60	40	–
PCL/TZ–HA	48	32	20

The wettability of the biomaterials was evaluated by contact angle measurements performed on a Contact angle System OCA20 (Dataphysics, Italy). A water droplet (1 μl) was poured on the surface of the biomaterials and the contact angle was measured by Software SCA20 (Dataphysics, Italy). Ten measurements for each composition were performed.

The biomaterials were subjected to degradation tests. Disc-shaped samples (10 mm in diameter and 1 mm thick) were placed in 24-well culture plates (1 sample/well) and soaked in 3 ml dH_2O at 37°C and the weight evolution measured at different times up to 60 days. Three samples were used for each composition and the degradation media changed every 3–4 days. For the morphological investigation, samples were dried and the surface and cross-section analyzed by scanning electron microscopy (SEM, LEICA S440) at an accelerating voltage of 20 kV, at various magnifications.

2.4 Rabbit mesenchymal stem cells (rMSCs) isolation and expansion

The adult MSCs were isolated from bone marrow of New Zealand White adult rabbits weighing approximately 3–4.5 kg. The bone marrow was harvested according to procedures described in details elsewhere [8]. Briefly, bone marrow was isolated from the distal and proximal left femur under sterile conditions and the aspirated material was settled in a tube containing sodium heparin (20 U ml^{-1} of aspirated material). Then, mononuclear cells were separated on Ficoll-Hystopaque 1077 gradients (Sigma–Aldrich, Saint Louis, Missouri, USA). The cells were washed and re-suspended at a density of 10^5 cells/ml in Mesencult basal medium containing MSC stimulatory supplements (Stemcell Technologies, Vancouver, Canada). Cells were then seeded in T12.5 flasks and incubated at 37°C, in a 5% CO_2 atmosphere and 95% of relative humidity. Adherent cells were allowed to reach approximately 80% confluence (12–17 days for the first passage). Cells were trypsinized and replaced every 6–8 days at approximately 80% confluence. The second passage (P2) of the cells was used if not otherwise stated. The animal experiments were performed in accordance with the institutional ethical protocol (No.116/92) for the protection of animal experimentations.

2.5 Subcultures of MSCs

When culture flasks were nearly confluent, the cells in the primary culture were detached by using trypsin-ethylenediaminetetraacetic acid (Gibco BRL, Grand Island, NY) and subcultured. For inducing osteogenesis, the medium

was replaced with the osteogenic differentiation medium (Differentiation Media BulletKits-Osteogenic; Cambrex, East Rutherford, NJ, USA) for 21 days. The cells were then collected for scaffold preparation.

2.6 Scaffold seeding and osteogenic differentiation of rMSC

2D non-porous scaffolds for cell culture experiments (10 mm in diameter and 2 mm thick) were γ-sterilized before seeding. For seeding, 2×10^4 cells, resuspended in 40 µl of medium, were statically seeded onto the different scaffolds. The scaffold/cell constructs were then placed in 24-well culture plates and incubated for 45 min in a humidified atmosphere (37°C, 5% CO_2) to allow for cell attachment. Cell-free medium (Mesencult medium) was then added to bring the total well volume to 1.5 ml. After incubation at 37°C for 24 h, the medium was replaced with osteogenic differentiation medium. MSCs control cultures were maintained in mesencult and osteogenic differentiation medium.

2.7 DNA quantification

Cell adhesion and proliferation were determined by DNA analysis. At predetermined time points, three replicate scaffolds were washed with phosphate-buffered saline (PBS) (Euroclone, Wetherby, UK) and transferred to centrifuge tubes containing 1 ml deionised, molecular-grade pure water. The tube were then transferred and stored at −20°C. After thawing, the samples were treated ultrasonically in an ice-water bath for 10 min and the released amount of DNA was measured from supernatant. Total amount of DNA was detected using Hoechst 33258 dye (Sigma–Aldrich, Italy). Sample fluorescence was measured with a luminescent spectrometer (LS50B, Perkin-Elmer, Waltham, USA) at an excitation and emission wavelengths of 360 and 460 nm, respectively. Samples were compared to the standard curve to determine the DNA content per composite.

2.8 Analysis for alkaline phosphatase activity

For ALP measurements, cells cultured in monolayers and scaffold–cell constructs after 21 days of culture were homogenized in 800 µl 0.1% Triton-X100 + 0.01% NaCl followed by sonication for 6 min. ALP activity was measured by using a biochemical assay (Sigma–Aldrich, Italy) based on conversion of *p*-nitrophenyl phosphatase to *p*-nitrophenol which was measured spectro-photometrically at 405 nm. ALP activity is expressed as micromoles of *p*-nitrophenol released. Scaffolds without cells served as control groups.

2.9 Detection and quantification of mineralization

Mineralized matrix synthesis was analyzed by ARS analysis. Cells cultured in monolayers and scaffold/cell constructs were washed with PBS (Euroclone) and fixed in 10% (v/v) formaldehyde (Sigma–Aldrich, Italy) at room temperature for 10 min. The monolayers and scaffold/cell constructs were then washed twice with excess dH_2O prior to addition of 1 ml of 40 mM ARS solution at pH 4.1 (Sigma–Aldrich, Italy). Samples were incubated at room temperature for 8 min in gentle shaking. After aspiration of the unincorporated dye, the wells were washed four times with 2 ml dH_2O while shaking for 5 min. The plates were stored at −20°C prior to dye extraction. Stained cell monolayers were visualized by inverted microscope. For quantification of staining, 800 µl 10% (v/v) acetic acid was added to the samples and plates were incubated in gentle shaking at room temperature for 30 min. Cell monolayers were removed by a scraper and transferred into microcentrifuge tube. Scaffold/cell constructs were sonicated in an ice-water bath sonicator for three times for 2 min and the supernatant was removed to a microcentrifuge tube. After vortexing, the slurry was overlaid with 500 µl mineral oil (Sigma–Aldrich, Italy), heated to 85°C for 10 min, and transferred to ice for 5 min. The slurry was centrifugated at 14,500 rpm for 15 min, the supernatants were collected in a new microcentrifuge tube. Then 200 µl of 10% ammonium hydroxide was added to each sample. Aliquotes (150 µl) of the supernatant were read in triplicate at 405 nm. Statistical analyses on three readings were carried out using Student's *t* test, and *P* values of less than 0.05 were considered significant. Scaffolds without cells served as control groups.

2.10 Semiquantitative RT-PCR measurements

The expression of the osteogenic marker, OPN, was evaluated by RT-PCR measurements. To isolate RNA, cells were lysed directly in the culture scaffold by adding 0.5 ml of TriReagent (Sigma–Aldrich, Italy). Total RNA was extracted according to the manufacturer's instructions. 2 µl of total RNA extracted were used for quantification by Standard Agilent 2100 bioanalyzer Agilent. 200 ng of total RNA for each sample was reverse transcribed using SuperScript RT (Gibco) and oligo dT priming. 5 µl aliquots of cDNA (50 ng equivalent of total RNA) were then amplified with specific primers in a Gene Amp PCR System 9600 thermocycler (Perkin-Elmer). PCR conditions were as follow: 11′ of initial denaturation at 94°C, and 30 cycles of 30″ at 94°C, 30″ at 57°C, 45″ at 72°C plus 7′ of final extension at 72°C. The following primers were used: OPN sense 5′-GCTCAGCACCTGAATGTACC-3′, OPN antisense 5′-CTTCGGCTCGATGGCTAGC-3′ (292-bp

product) GAPDH sense 5′-TCATTTGAAGGGCGGAG CCAA-3′, GAPDH antisense 5′-ATGCCTGCTTCACCA CCTTCT-3′ (465-bp product). All primer sequences were exon/intron overspanning to prevent possible signals from genomic DNA. PCR conditions and the number of PCR cycles for each primer pair (30 cycles for GAPDH and OPN) were chosen according to preliminary experiments in which the PCR product was detectable in an amount directly proportional to the quantity of starting cDNA. RT-PCR products were electrophoresed on 2% agarose gel stained with ethidium bromide and run with a 100 bp ladder to confirm the predicted size. Relative levels of each PCR product were quantified by densitometric analysis of gel photographs using the Quantity One software and normalized to the signal from the housekeeping gene GAPDH. The ratio between the OPN RNA and GAPDH was calculated to normalize for initial variations in sample concentration and as a control for reaction efficiency. Scaffolds without cells served as control groups.

2.11 Preliminary investigation about the design of 3D porous scaffolds via gas foaming technique

The design of 3D porous scaffolds starting from the multi-phase PCL/TZ and PCL/TZ–HA biomaterials was investigated by using the gas foaming technique [21]. Disc-shaped samples (d = 10 mm and h = 2 mm) were solubilized with CO_2 at 150 MPa and 70°C for 4 h in a batch foaming apparatus [21]. After solubilization, the system was brought to the desired foaming temperature (T_F) and the pressure was quenched to atmosphere to allow for samples foaming. $T_F = 44$°C was selected for the PCL/TZ sample, while $T_F = 100$°C for PCL/TZ–HA. To stabilize the pore structure, foams were immediately cooled down to ambient temperature and subsequently removed from the vessel.

The morphology of the scaffolds was assessed by Scanning Electron Microscope (SEM, LEICA S440) analysis, while the pore size was calculated by image analysis, according to ASTM D3576. In particular, the SEM micrographs were converted to binary images and then analyzed by Image J® software in order to evaluate the pore size distribution of the scaffolds. At least 100 pores were analyzed for each scaffold type.

3 Results

3.1 TGA

Figure 1a and b reported the TGA and differential TGA (DTGA) curves of the different biomaterials. DTGA curve of PCL/TZ showed three peaks. The first peak at 100°C

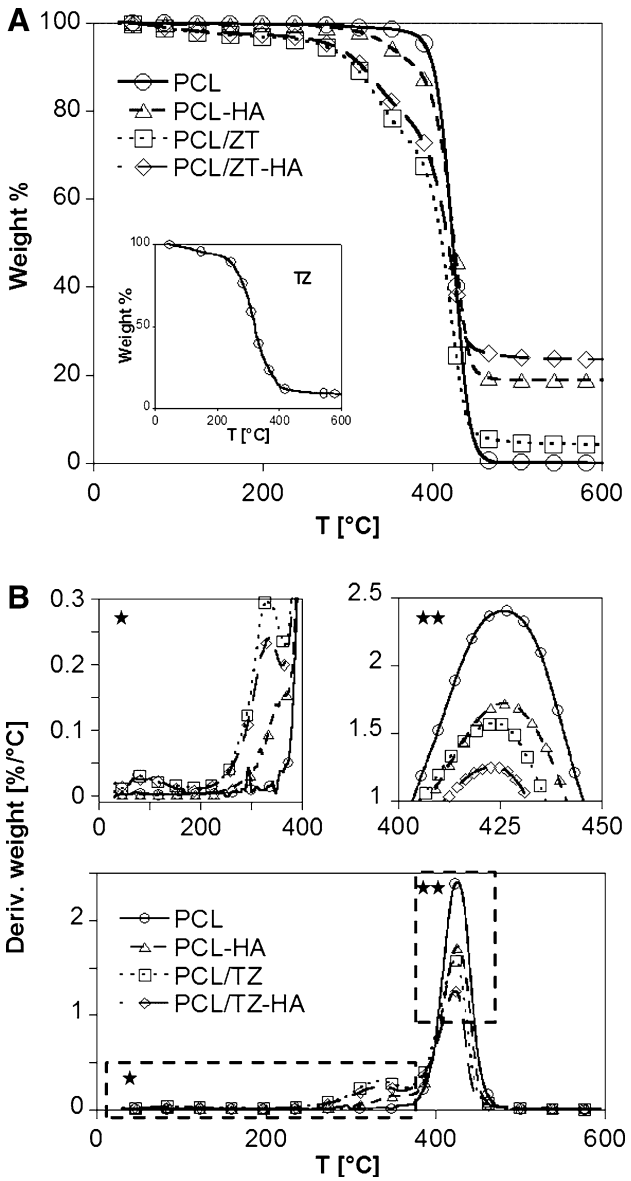

Fig. 1 TGA/DTGA curves of the different biomaterials. The *inset* of (**a**) reported the TGA curve of neat TZ

was attributed to the evaporation of the water and low molecular weight compounds, such as PEG molecules, of the TZ phase (* inset of Fig. 1b). The second and third peaks, at 330 and 410°C ca., can be attributed to the thermal degradation of the TZ (inset of Fig. 1a) and PCL, respectively [16, 21], this result proving the heterogeneous nature of the blend. The addition of the HA resulted in the presence of a residual weight at 600°C of about 20 wt% for the PCL–HA, equal to the concentration of the inorganic filler into the polymeric matrix (Fig. 1a). Furthermore, the TZ does not degrade completely at the final test temperature [21], as observed in the case of PCL/TZ thermogram, where a residue of 4 wt% ca. at 600°C was present (Fig. 1a). PCL/TZ–HA blend, accordingly, had a final

residue at 600°C of 24%. Nevertheless, with respect to neat PCL, the multi-phase PCL/TZ–HA composite showed a 3°C decrease in the maximum of the temperature of the third degradation peak (** inset of Fig. 1b), evidencing a slight decrease in the thermal stability of PCL when mixed to the other components.

3.2 DMA

Damping factor (tan δ) versus temperature curves of the different biomaterials were reported in Fig. 2. The PCL and PCL–HA showed only one peak, at −60°C ca. related to the glass transition temperature of PCL (see Sect. 2.1). Conversely, PCL/TZ and PCL/TZ–HA curves were characterized by two different peaks, at −60 and 40°C ca., corresponding to the glass transition temperatures of PCL and TZ, respectively. This consideration was supported by the tan δ peak at 40°C, for neat TZ (inset of Fig. 2). TGA and DMA analyses demonstrated that, after blending, the two polymers formed a multi-phase system due to their different chemical nature [22].

3.3 Tensile properties

The σ_Y, ε_B and σ_B of the different biomaterials are reported in Table 2. With respect to pure PCL, the multi-phase PCL/TZ blend was characterized by reduced deformability, as demonstrated by the decrease of two orders of magnitude of ε_B, from 9.2 ± 1.5 to 0.095 ± 0.03 mm/mm (Table 2). Similar behaviour was also observed when the HA was incorporated within PCL and PCL/TZ blend, even if, in this case, the effect was less pronounced.

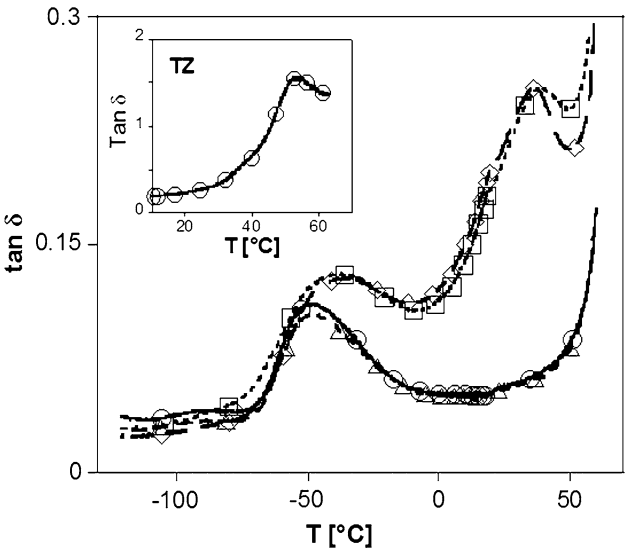

Fig. 2 Tan δ vs. temperature curves for the different biomaterials. The *inset* reported the tan δ vs. temperature curve of neat TZ

Table 2 Tensile properties of different biomaterials ($n = 5$)

Scaffold	σ_Y (MPa)	ε_B (mm/mm)	σ_B (MPa)
PCL	22.5 ± 1.2	9.17 ± 1.5	44.7 ± 3.1
PCL–HA	17.28 ± 0.65	1.02 ± 0.09	16.25 ± 0.86
PCL/TZ	10.87 ± 0.085	0.095 ± 0.03	9.01 ± 0.182
PCL/TZ–HA	7.68 ± 0.34	0.052 ± 0.013	6.92 ± 0.36

σ_Y, σ_B and ε_B are the yielding stress, the stress at break and the elongation at break, respectively

3.4 Wettability and in vitro degradation

The results of the wettability tests are reported in Fig. 3. We observed that, with respect to pure PCL, the addition of TZ enhanced the wettability of the system, as indicated by the decrease of the contact angle from 82.5 ± 5.5 to 72.2 ± 1.6. Furthermore, the contact angle values of PCL–HA (equal to 83.9 ± 6.5) and PCL/TZ–HA composites (equal to 72.7 ± 3.1) were close to those observed for PCL and PCL/TZ, respectively, indicating a minor effect of HA particles on the wettability. Conversely, topography changed with the inclusion of HA, since the roughness of the surface of the composites, as shown in Fig. 3b and d, increased considerably.

The effect of scaffold formulation on the weight evolution during degradation in water at 37°C is reported in Fig. 4. The weight of PCL and PCL–HA remained almost unchanged during the test, while significant differences were observed for PCL/TZ and PCL/TZ–HA. In particular, these samples showed a rapid water absorption, with the maximum weight measured at day 1, followed by the progressive weight decrease over time. This effect was more pronounced for the PCL/TZ blend rather than the PCL/TZ–HA composite and, indicated a reduced swelling and degradation phenomena as a consequence of HA introduction.

The SEM micrographs of the PCL/TZ and PCL/TZ–HA before and after the degradation are reported in Fig. 5. Before degradation (Fig. 5a, b), we observed an almost compact surface, with the PCL/TZ–HA composite characterized by enhanced surface roughness (high magnifications reported in the insets of Fig. 5a, b). Furthermore, in agreement with the results reported in Fig. 4, the in vitro degradation significantly affected the morphology of the multi-phase systems. In particular, a limited porosity was observed on the PCL/TZ surface after 19 days of degradation (Fig. 5c), while larger voids were detected onto the surface of the PCL/TZ–HA composite at the same degradation time (Fig. 5d). The cross-sections of the multi-phase systems reported in Fig. 5e and f also showed the presence of some porosity within the samples. In particular, the larger pores

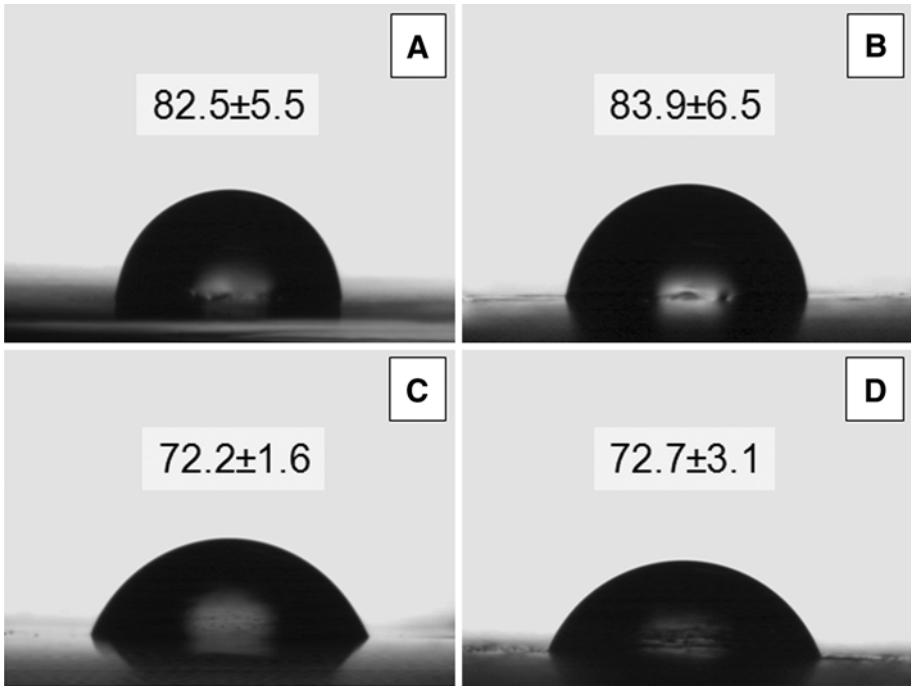

Fig. 3 Contact angle measurements of **a** PCL; **b** PCL–HA; **c** PCL/TZ and **d** PCL/TZ–HA

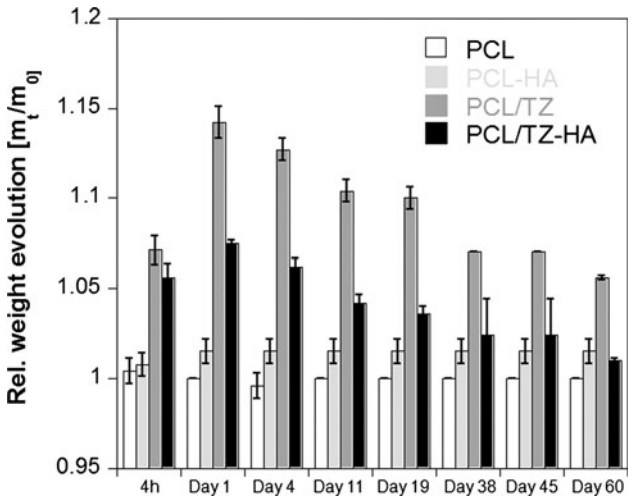

Fig. 4 Effect of biomaterial formulation on relative weight evolution during degradation test at 37°C (m_t = wet weight, m_0 = initial weight)

observed in Fig. 5e may be ascribed to the phase separated nature of the system and to the faster degradation of the TZ phase if compared to the PCL. Furthermore, the formation of tiny pores was observed in the degraded TZ phase, as indicated by the black arrows of Fig. 5e (higher magnification). Finally, Fig. 5f showed the submicron porosity of the HA granules, responsible for an enhanced adhesion with the surrounding polymer. It is important to note that, after 60 days of degradation, the PCL/TZ and PCL/TZ–HA loosed up to 13% of their initial dry weight.

3.5 Establishment of primary cultures and osteogenic differentiation

Cells obtained from rabbit bone marrow were cultured as described in the previous section and, after 15 days of culture, an almost homogeneous population of fibroblast-like cells was observed throughout the flask, with little evidence of round or floating cells. These cells were induced to differentiate into various lineages and were able to proliferate in vitro for a long time. The capacity to proliferate is maintained until the 30th passage, although the capacity to differentiate is reduced as the passage number increases. Because of their proliferative and differentiative abilities we refer to these cells as rMSCs. These rMSCs were plated and treated for osteogenic differentiation for 21 days. Osteogenic differentiation was evaluated in both standard and osteogenic culture media. Proliferation and differentiation of control cells and osteoblastic medium cultures were compared using phase contrast microscopy. After 7 days of culture, nodular aggregates became evident for cells cultured in osteogenic medium and their amount increased after 21 days of culture (Fig. 6b). As evidenced by the ARS results of Fig. 6d, these aggregates were characterized by calcium deposits. Similar aggregates were observed for control cell cultures, but, in this case, they were smaller and clearly evident only after 14 days of culture. Furthermore, no evidence of calcium deposition was observed for cells cultured under standard conditions, even at 21 days of culture (Fig. 6a, c). These results were confirmed by those of the total calcium content and

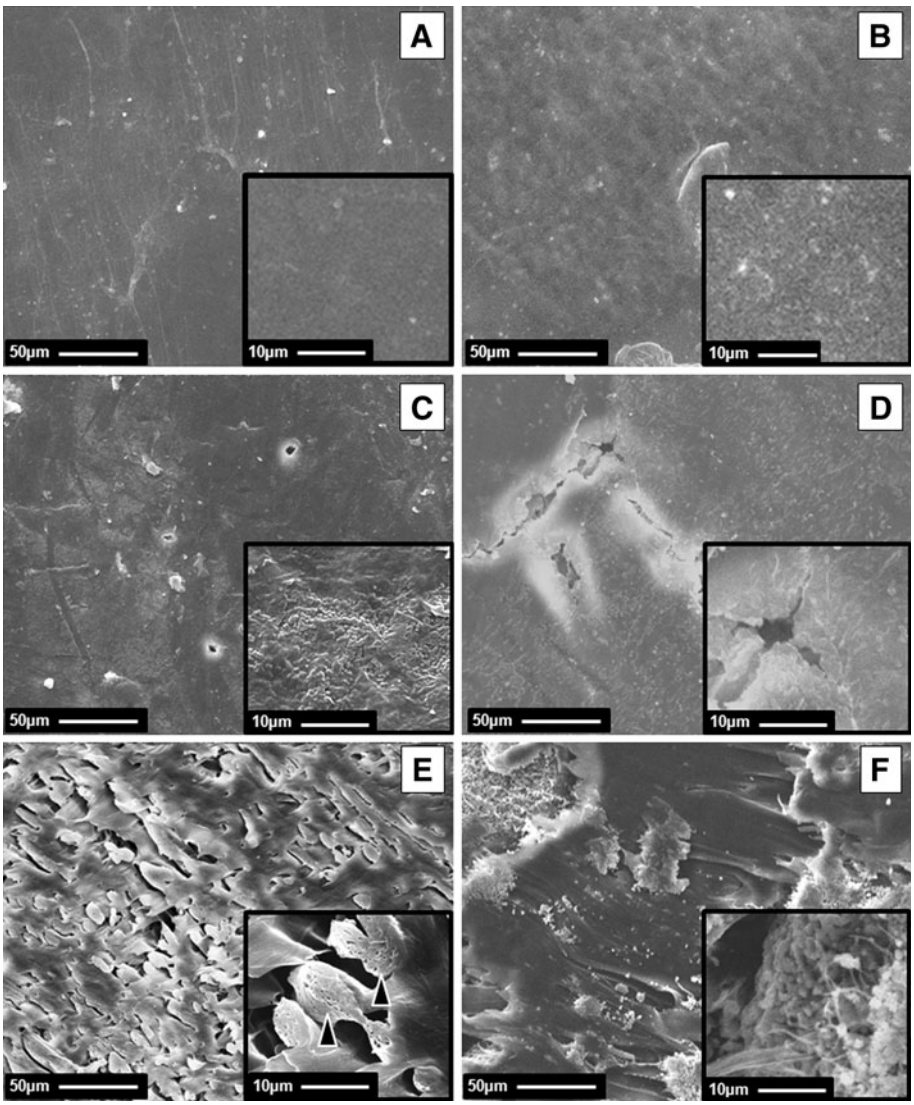

Fig. 5 SEM micrographs of **a** PCL/TZ and **b** PCL/TZ–HA surfaces; SEM micrographs of surface (**c** and **d**) and cross-section (**e** and **f**) of PCL/TZ and PCL/TZ–HA, respectively, after 19 days of degradation. The *black arrows* indicated the porosity induced into the TZ phase by the degradation process

ALP activity reported in Fig. 6e and f, respectively, evidencing enhanced osteogenic expression and calcium deposition for rMSCs cultured under osteogenic conditions.

3.6 In vitro assessment of rMSCs adhesion, proliferation and differentiation on the scaffolds

The rMSCs were used in order to characterize the biological response of the different biomaterial scaffolds. DNA was extracted from the scaffold/cell constructs to evaluate cell adhesion and proliferation and the results reported in Fig. 7a. If compared to the neat PCL, the incorporation of TZ and HA resulted in an enhancement of both cell adhesion (DNA data at day 1) and proliferation. This effect was more evident for the PCL/TZ–HA, for which a significantly higher cell number was observed at day 7 and day 21 ($n = 5$, $P < 0.05$) (Fig. 7a). The osteogenic expression of the rMSCs was assessed by ALP, ARS and OPN quantification at 21 days of culture under osteogenic medium. As shown in Fig. 7b, the ALP activity of the osteogenically induced rMSCs cultured onto the PCL/TZ–HA scaffold was significantly higher than the activity of the cells cultured on PCL, PCL–HA and PCL/TZ scaffolds ($n = 6$ $P < 0.05$). Similarly, higher calcium deposition was found for the PCL/TZ–HA scaffold compared to the other scaffolds (Fig. 7c). These results were also confirmed by those of the transcript expression of osteogenic and condrogenic differentiation markers evaluated by semiquantitative RT-PCR analysis. Indeed, if compared to neat PCL, a fourfold increase in OPN transcript level was observed for the hMSCs cultured onto the PCL/TZ–HA scaffold after 21 days of culture (Fig. 7d).

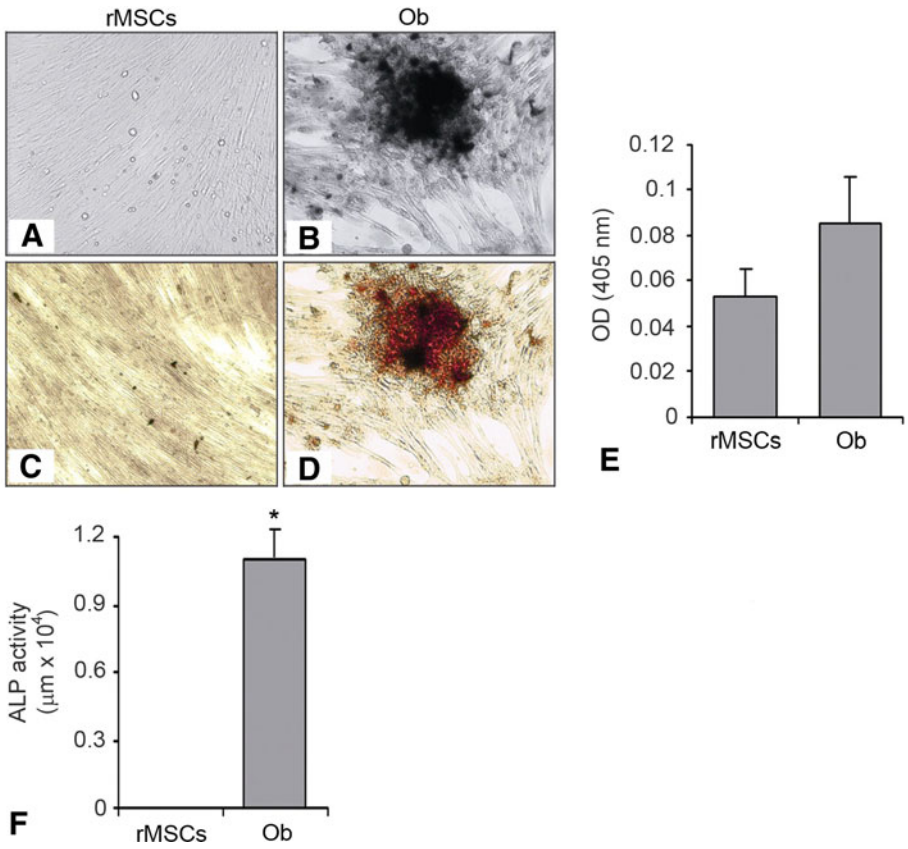

Fig. 6 rMSCs after 21 days of induction. **a** rMSCs culture treated with culture medium alone; **b** rMSCs culture treated with the osteogenic medium rMSCs; **c** rMSCs treated with medium alone and **d** with osteogenic medium stained with alizarin red. **e** Total calcium in cells treated with osteogenic medium with respect to cells treated with medium alone. * Statistically significant differences ($P < 0.05$). **f** ALP activity assay**.** ALP activity was evaluated in cells treated in osteogenic medium with respect to cells treated with culture medium alone; expressed as μmol thymolphthalin/mg protein

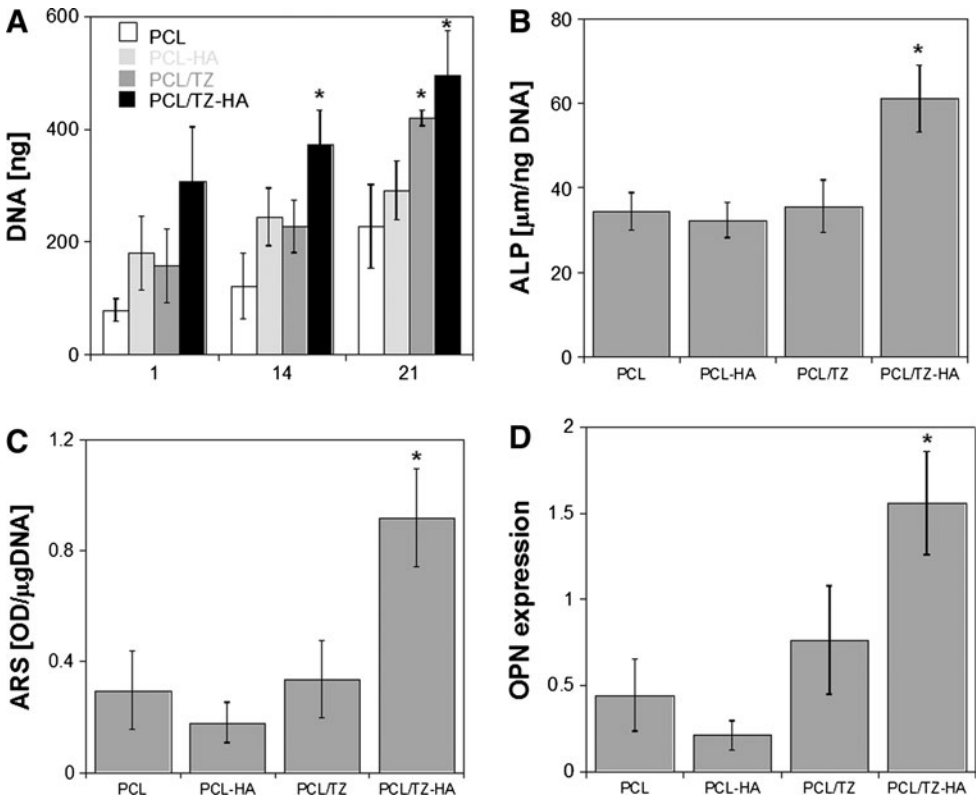

Fig. 7 **a** Total protein content expressed as a mg protein/ml at 24 h, day 7 and day 21. **b** ALP/DNA activity at 21 days. **c** ARS/DNA results. **d** Transcript expression of OPN-differentiation markers quantified by semi-quantitative RT-PCR. Transcript levels were normalized to GAPDH within the linear range of amplification. All of the data are reported as mean ± standard deviation ($n = 5$) and were normalized to scaffold control group

3.7 3D porous scaffolds design by gas foaming

In order to assess the versatility of the multi-phase systems prepared for bone tissue engineering, we investigated the fabrication of 3D porous scaffolds by the gas foaming technology [21, 23]. The scaffolds were prepared by using CO_2 as blowing agent and performing the foaming process at 44°C for the PCL/TZ sample and at 100°C for the PCL/TZ–HA one. Microscope images of PCL/TZ and PCL/TZ–HA samples before and after foaming are reported in Fig. 8a and b, as well as the pore size distributions in Fig. 8c. The visual observation of the foamed systems evidenced significant morphological changes after foaming, while samples maintained their disc-shaped geometry (Fig. 8a, b). However, with respect to the unfoamed samples (Fig. 5a, b), both the PCL/TZ and PCL/TZ–HA scaffolds showed a pore structure induced by the nucleation and growth of the gas bubbles during the foaming process (SEM micrographs of Fig. 8a, b). By comparing the pore size distributions of the foams, reported in Fig. 8c, we observed significant differences between the PCL/TZ and PCL/TZ–HA systems. In particular, the PCL/TZ–HA was characterized by smaller pores and a narrower pore size distribution if compared to the PCL/TZ.

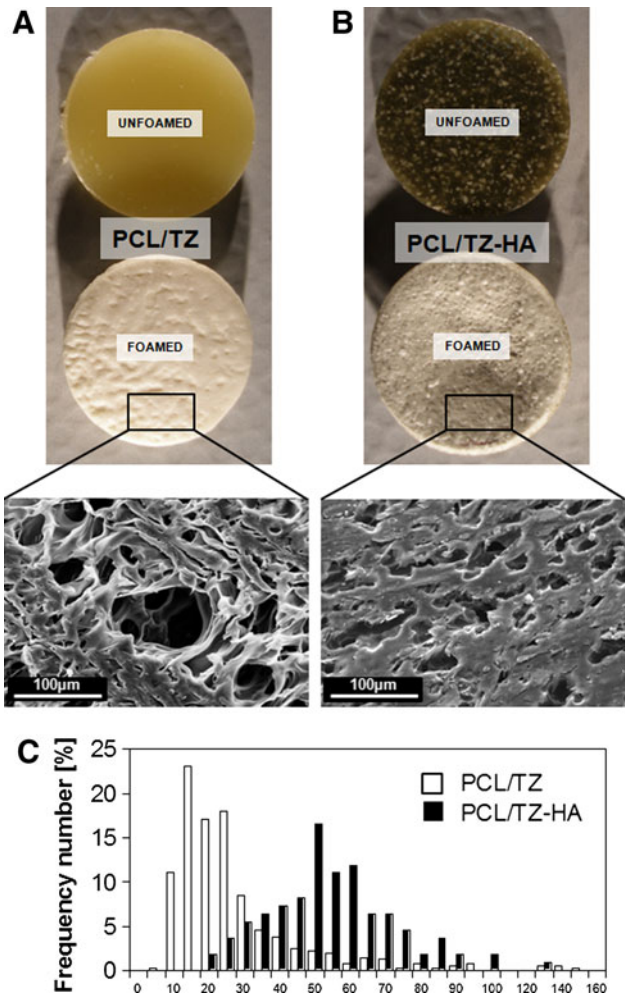

Fig. 8 Optical and SEM microscope images of **a** PCL/TZ and **b** PCL/TZ–HA before and after the gas foaming step; **c** pore size distributions of the porous PCL/TZ and PCL/TZ–HA scaffolds prepared by the gas foaming process

4 Discussion

The challenge of bone-tissue engineering is the design of a scaffold that is capable of mimicking the natural properties of bone while providing a temporary substrate for tissue regeneration [3, 4, 6]. The scaffold must be composed of an osteoconductive material which mimics the calcified matrix of bone and incorporates the necessary bioactive factors to make it osteoinductive [24]. Furthermore, this material must be characterized by degradation and resorption rates that match cell/tissue growth in vivo [4].

In the current study, we described the preparation, micro-structural characterization and biological response of novel multi-phase polymer/ceramic composite biomaterials with potential applications in bone tissue engineering. In particular, this study was devoted to characterize the micro-structural properties, hydrophilicity and degradation of multi-phase biomaterials, finally aiming to the selection of the best composition for bone regeneration. To this ultimate goal, we evaluated the 2D rMSCs adhesion, proliferation and osteogenic differentiation in vitro.

4.1 Physical properties and in vitro degradation of the biomaterials

The PCL, TZ and HA components selected for the preparation of the biomaterials were melt-mixed by using the composition reported in Table 1. Differently from the bioartificial blends prepared by dispersing a natural polymer within a thermoplastic synthetic matrix [15], our systems were obtained by blending two immiscible thermoplastic materials. The results of the TGA and DMA analyses reported in Figs. 1 and 2 showed that the PCL/TZ blend and PCL/TZ–HA composite were characterized by heterogeneous multi-phases micro-structures. In particular we observed the presence of two thermal degradation peaks (Fig. 1) and glass transition temperatures (Fig. 2). The presence of an heterogeneous micro-structure is an important aspect from a technological and biomedical point of view. For instance, the higher relaxation temperature of the PCL/TZ and PCL/TZ–HA (Fig. 2), close to the human body temperature, may allow for the dissipation of a cyclic mechanical solicitation with time scales of the order of 1 s, especially at the early stage of application [25].

As reported in Fig. 2 and Table 2, the HA particles did not significantly affect the miscibility of the two polymers, while they influence their mechanical behavior [26]. In particular, we observed the decrease of the ductility of the HA-based composites, as evidenced by the significant reduction of ε_B. This effect may be ascribed to several factors, such as filler size and concentration as well as to the low compatibility between PCL and HA [26, 27]. Similar results were observed when PCL was blended with TZ, as also reported by Shin et al. for PCL/thermoplastic starch blends [28].

Parameters such as surface topography and wettability strongly influence MSCs adhesion, proliferation and differentiation [29, 30]. The results of the contact angle measurements and water degradation tests, reported in Figs. 3 and 4, are in agreement with those reported by Tan and Teoh for PCL film [31] and by Shi et al. for zein film [32], demonstrating that the TZ enhanced the wettability of PCL. Conversely, the HA particles enhanced both the roughness and, to a minor extent the wettability of the scaffolds surface (Figs. 3 and 5), resulting in the concomitant modification of scaffold topography and hydrophilicity. The faster degradation rates observed for the PCL/TZ and PCL/TZ–HA (Figs. 4 and 5) may be explained by considering that the TZ may possess the ability to swell and degrade in water. Indeed, even if zein is almost insoluble in water [17, 18], when thermo-plasticized with PEG, it was able to swell and partially dissolve in water, as a consequence of the lubricant effect of PEG and due to the higher hydrophilic nature and solubility of the plasticizer in aqueous environments. This consideration is in agreement with the results of the morphological analysis reported in Fig. 5, which showed the morphology of the PCL/TZ and PCL/TZ–HA at different degradation times. The composition of the blends, close to the phase inversion point (Table 1) [22, 23], allowed for the formation of co-continuous micro-structures and, therefore, the constant exposure of the two different polymeric materials to the degradation medium. As a direct consequence, we observed a faster degradation of the multi-phase systems and, consequently, the formation of a porosity on the surface (Fig. 5c, d) and into the interior (Fig. 5e, f) of the PCL/TZ and PCL/TZ–HA samples.

4.2 Cell/material interaction

The multilineage potential of bone marrow-derived precursor cells, their relative availability in terms of cell harvesting and their capacity to undergo extensive replication without a loss of multipotential capacity make them an attractive cell source for bone regeneration [6, 8]. From a biomedical point of view it is important to design scaffolds which provide a bioactive environment, leading to improved cell proliferation, differentiation and biosynthesis.

As reported in Fig. 6, when rMSCs were exposed to osteogenic medium, they changed their phenotype, as compared with control cells. Indeed, differently from the control (Fig. 6a, c, e), we observed extensive rMSCs mineralization under osteogenic medium, with the formation of calcium aggregates after 21 days of culture (Fig. 6b, d, e). ALP immunostaining confirmed these results, showing the expression of osteogenic markers for cell culture under differentiation medium at day 21 (Fig. 6f). These results are consistent with those reported by Schantz et al. [6], proving the osteogenic potential of rMSCs when cultured under osteogenic medium conditions.

The number of cells of the scaffold/cell constructs at different culture times was determined by measuring DNA content and assessing rMSCs proliferation during the incubation period. As evidenced by the DNA values at 24 h from seeding, the highest cell adhesion was achieved for the PCL/TZ–HA, as evidenced by the fourfold increase in the number of cells onto the PCL/TZ–HA, if compared to neat PCL, at day 1 (Fig. 7a). Furthermore, rMSCs proliferated on all of the scaffold surfaces, with a significantly higher cell number on the PCL/TZ–HA composite scaffold (Fig. 7a).

The ability of a scaffold to support and promote MSCs adhesion and proliferation is strongly dependent on its chemistry and topography [29, 30, 33, 34]. For instance, the hydrophobic surface of PCL scaffolds may be detrimental to the achievement of optimal seeding efficiency and may also hinder the proliferation activity of osteogenic cells [14]. Furthermore, it has been recently demonstrated that cell adhesion was promoted on rough surfaces with respect to smooth ones [30, 33]. Albeit the difficulty of discriminating between the effect of the different physical–chemical parameters on the scaffold/cell interaction, the enhanced rMSCs adhesion and proliferation observed on the PCL/TZ–HA scaffold may be mainly attributed to the improved hydrophilicity and surface roughness of this scaffold (Figs. 3 and 5) [14, 29, 30, 33, 34].

The differentiation of MSCs is one of the key step in the process of bone regeneration. ALP expression is an early marker of osteoblast maturation and therefore, it is one of the most used osteogenic markers. [6, 9, 13]. As also evidenced for cell proliferation, the osteogenic differentiation of rMSCs on the scaffolds was strongly affected its composition. In particular, our results indicated that the ALP activity of the cells seeded on the PCL/TZ–HA scaffold at 21 days of culture was up to two times higher than that of the others systems investigated. Similar results were also achieved for the OPN expression (Fig. 7d) and for the total calcium deposition (Fig. 7c), finally indicating that, among the bone scaffolds prepared, the PCL/TZ–HA composite

was the most efficient. These results suggest that, when combined in a unique PCL/TZ–HA multi-phase system, PCL, TZ and HA may act in a synergistic fashion and enhanced the osteogenic expression and calcium deposition of rMSCs. One of the possible explanation of this effect may be the increased hydrophilicity and degradation rate of the TZ, if compared to PCL (Figs. 3 and 5), that may enhance the absorption of serum proteins and the exposure of the HA particles, too, finally promoting the rMSCs osteogenic differentiation [14]. At the same time, TZ and HA also affected the topography of the scaffold surface and, in turn, may have had a great impact on cell adhesion, proliferation and osteogenic differentiation [14, 33]. All of these results demonstrated the enhanced osteogenic properties of the multi-phase PCL/TZ–HA biomaterial.

4.3 3D porous scaffolds design by gas foaming

The majority of bone tissue engineering applications for the regeneration of 3D tissues requires the design of biocompatible and biodegradable scaffolds which are also porous [3, 4, 10, 11]. Indeed, porosity is often essential to mimic the micro-environment of the native tissue, to allow for cell invasion and infiltration as well as for nutrients and metabolic wastes transport in 3D [3, 4, 10, 11]. The morphological characterization reported in Fig. 8 demonstrated the possibility to designing porous scaffolds starting from the multi-phase PCL/TZ and PCL/TZ–HA biomaterials, by the gas foaming technique. The SEM micrographs of the scaffolds after foaming evidenced the presence of quite homogeneous pore structures, as well as the decrease of the pore size distribution for the PCL/TZ–HA sample, if compared to the PCL/TZ one. Although the biomaterials were foamed at different T_F, 44°C for the PCL/TZ and 100°C for the PCL/TZ–HA, this difference may be ascribed in part to the increase of the stiffness of the polymeric matrix after the incorporation of the HA particles and, therefore, the decrease of its foamability [35]. Nevertheless, even if the pore size distributions of the scaffolds were too small for bone tissue engineering (Fig. 8c) [3, 4], this preliminary investigation demonstrated that the proposed multi-phase systems may be further processed in order to prepare 3D porous scaffolds.

5 Conclusions

In this work we characterized the in vitro degradation and biological response of novel multi-phase biomaterials for use in bone regeneration applications.

When melt blended with TZ and HA, PCL formed multi-phase systems with enhanced wettability and degradation. The results of the cell–scaffold interaction study suggested a key role of the composition of the systems on rMSCs adhesion, proliferation and osteogenic expression. In particular, the PCL/TZ–HA composite proved the most interesting biomaterial for bone tissue engineering application purpose.

Finally, the proposed multi-phase biomaterials were successfully processed via the gas foaming technology in order to produce 3D porous scaffolds.

Acknowledgements This research has been financially supported by a grant of the Italian Ministry of Health, art. 12bis D. Lgs. 229/99. The authors thank Finceramica (Faenza) for supply the HA used in this work.

References

1. Mercuri LG. Alloplastic temporomandibular joint reconstruction. Oral Surg Oral Med Oral Pathol Oral Radiol Endod. 1998; 85:631–7.
2. Warnke PH, Springer ING, Wiltfang J, Acil Y, Eufinger H, Wehmöller M, Russo P, Bolte H, Sherry E, Behrens E. Growth and transplantation of a custom vascularised bone graft in a man. Lancet. 2004;364:766–70.
3. Salgado AJ, Coutinho OP, Reis RL. Bone tissue engineering: state of the art and future trends. Macromol Biosci. 2004;4:743–65.
4. Hutmacher DW. Scaffolds in tissue engineering bone and cartilage. Biomaterials. 2000;21:2529–43.
5. Eppley BL, Platis JM, Sadove AM. Experimental effects of bone plating in infancy on craniomaxillofacial skeletal growth. Cleft Palate Craniofac J. 1993;30:164–9.
6. Schantz JT, Teoh SH, Lim TC, Endres M, Lam CX, Hutmacher DW. Repair of calvarial defects with customized tissue-engineered bone grafts I. Evaluation of osteogenesis in a three-dimensional culture system. Tissue Eng. 2003;9:113–26.
7. Caplan AL. Adult mesenchymal stem cells for tissue engineering versus regenerative medicine. J Cell Physiol. 2007;213:341–7.
8. Kadiyala S, Jaiswal N, Bruder SP. Culture-expanded, bone marrow-derived mesenchymal stem cells can regenerate a critical-sized segmental bone defect. Tissue Eng. 1997;3:173–85.
9. Mygind T, Stiehler M, Baatrup A, Li H, Zou X, Flyvbjerg A, et al. Mesenchymal stem cell ingrowth and differentiation on coralline hydroxyapatite scaffolds. Biomaterials. 2007;28(6): 1036–47.
10. Woodard JR, Hilldore AJ, Lan SK, Park CJ, Morgan AW, Eurell JAC, Clark SG, Wheeler MB, Jamison RD, Johnson AJW. The mechanical properties and osteoconductivity of hydroxyapatite bone scaffolds with multi-scale porosity. Biomaterials. 2007; 28:45–54.
11. Ma PX, Zhang R, Xiao G, Franceschi R. Engineering new bone tissue in vitro on highly porous poly(a-hydroxyl acids)/hydroxyapatite composite scaffolds. J Biomed Mater Res. 2001; 54:284–93.
12. Murugan R, Ramakrishna S. Development of nanocomposites for bone grafting. Compos Sci Technol. 2005;65:2385–406.
13. Shor L, Güçeri S, Wen X, Gandhi M, Sun W. Fabrication of three-dimensional polycaprolactone/hydroxyapatite tissue scaffolds and osteoblast–scaffold interactions in vitro. Biomaterials. 2007;28:5291–7.
14. Kim S, Ahn K, Park MS, Lee J, Choi CY, Kim B. A poly(lactide-*co*-glycolide)/hydroxyapatite composite scaffold with enhanced osteoconductivity. J Biomed Mater Res. 2007;80A:206–15.

15. Ciardelli G, Chiono V, Vozzi G, Pracella M, Ahluwalia A, Barbani N, et al. Blends of poly-(ε-caprolactone) and polysaccharides in tissue engineering applications. Biomacromolecules. 2005;6:1961–76.
16. Di Franco CR, Cyras VP, Busalmen JP, Ruseckaite RA, Vázquez A. Degradation of polycaprolactone/starch blends and composites with sisal fibre. Polym Degrad Stab. 2004;86:95–103.
17. Dong J, Sun Q, Wang J. Basic study of corn protein, zein, as a biomaterial in tissue engineering, surface morphology and biocompatibility. Biomaterials. 2004;25:4691–7.
18. Gong S, Wang H, Sun Q, Xue S, Wang J. Mechanical properties and in vitro biocompatibility of porous zein scaffolds. Biomaterials. 2006;27(20):3793–9.
19. Van Vlierberghe S, Cnudde V, Dubruel P, Masschaele B, Cosijns A, De Paepe I, Jacobs PJS, Van Hoorebeke L, Remon JP, Schacht E. Porous gelatin hydrogels. 1. Cryogenic formation and structure analysis. Biomacromolecules. 2007;8:331–7.
20. Vandelli MA, Rivasi F, Guerra P, Forni F, Arletti R. Gelatin microspheres crosslinked with D,L-glyceraldehyde as a potential drug delivery system: preparation, characterisation, in vitro and in vivo studies. Int J Pharm. 2001;215:175–84.
21. Salerno A, Oliviero M, Di Maio E, Iannace S. Thermoplastic foams from zein and gelatin. Int Polym Proc. 2007;22(5):480–8.
22. Marin S, Favis BD. Co-continuous morphology development in partially miscible PMMA/PC blends. Polymer. 2002;43:4723–31.
23. Salerno A, Oliviero M, Di Maio E, Iannace S, Netti PA. Design of porous polymeric scaffolds by gas foaming of heterogeneous blends. J Mater Sci: Mater Med. 2009;20(10):2043–51.
24. Ishaug-Riley SL, Crane GM, Gurlek A, Miller MJ, Yasko AW, Yaszemski MJ. Ectopic bone formation by marrow stromal osteoblast transplantation using poly(DL-lactic-*co*-glycolic acid) foams implanted into the rat mesentery. J Biomed Mater Res. 1997;36:1–8.
25. Mano JF, Reis RL, Cunha AM. Effects of moisture and degradation time over the mechanical dynamical performance of starch-based biomaterials. J Appl Polym Sci. 2000;78:2345–57.
26. Kim H. Biomedical nanocomposites of hydroxyapatite/polycaprolactone obtained by surfactant mediation. J Biomed Mater Res. 2007;83A:169–77.
27. Azevedo MC, Reis RL, Claase MB, Grijpma DW, Feijen J. Development and properties of polycaprolactone/hydroxyapatite composite biomaterials. J Mater Sci Mater Med. 2003;14:103–7.
28. Shin B, Lee S, Shin Y, Balakrishanan S, Rayan R. Rheological, mechanical and biodegradation studies on blends of thermoplastic starch and polycaprolactone. Polym Eng Sci. 2004;44:1429–38.
29. Chastain SR, Kundu AK, Dhar S, Calvert J, Putnam AJ. Adhesion of mesenchymal stem cells to polymer scaffolds occurs via distinct ECM ligands and controls their osteogenic differentiation. J Biomed Mater Res. 2006;78A:73–85.
30. Neuss S, Apel C, Buttler P, Denecke B, Dhanasingh A, Ding X, et al. Assessment of stem cell/biomaterial combinations for stem cell-based tissue engineering. Biomaterials. 2008;29:302–13.
31. Tan PS, Teoh SH. Effect of stiffness of polycaprolactone (PCL) membrane on cell proliferation. Mater Sci Eng C. 2007;27:304–8.
32. Shi K, Kokini JL, Huang Q. Engineering zein films with controlled surface morphology and hydrophilicity. J Agric Food Chem. 2009;57:2186–92.
33. Lange R, Lüthen F, Beck U, Rychly J, Baumann A, Nebe B. Cell–extracellular matrix interaction and physico-chemical characteristics of titanium surfaces depend on the roughness of the material. Biomol Eng. 2002;19:255–61.
34. Marletta G, Ciapetti G, Satriano C, Perut F, Salerno M, Baldini N. Improved osteogenic differentiation of human marrow stromal cells cultured on ion-induced chemically structured poly-ε-caprolactone. Biomaterials. 2007;28(6):1132–40.
35. Salerno A, Iannace S, Netti PA. Open-pore biodegradable foams prepared via gas foaming and microparticulate templating. Macromol Biosci. 2008;8:655–64.